Click Here for Full Article

Depletion of perennial sea ice in the East Arctic Ocean

S. V. Nghiem,[1] Y. Chao,[1] G. Neumann,[1] P. Li,[1] D. K. Perovich,[2] T. Street,[3] and P. Clemente-Colón[3]

Received 19 June 2006; revised 12 July 2006; accepted 18 July 2006; published 7 September 2006.

[1] The extent of perennial sea ice in the East Arctic Ocean (0–180°E) decreased by nearly one half with an abrupt reduction of 0.95×10^6 km^2, while the West Arctic Ocean (0–180°W) had a slight gain of 0.23×10^6 km^2 between 2004 and 2005, as observed by satellite scatterometer data during November–December. The net decrease in the total perennial ice extent is 0.72×10^6 km^2, about the size of Texas. Perennial ice in the East Arctic Ocean continued to be depleted with an areal reduction of 70% from October 2005 to April 2006. With the East Arctic Ocean dominated by seasonal sea ice, a strong summer melt may open a vast ice-free region with a possible record minimum ice extent largely confined to the West Arctic Ocean. Simultaneous scatterometer measurements of sea ice and winds will be crucial for sea ice monitoring and forecasts. **Citation:** Nghiem, S. V., Y. Chao, G. Neumann, P. Li, D. K. Perovich, T. Street, and P. Clemente-Colón (2006), Depletion of perennial sea ice in the East Arctic Ocean, *Geophys. Res. Lett.*, *33*, L17501, doi:10.1029/2006GL027198.

1. Introduction

[2] Arctic sea ice has undergone anomalous change in the past decade. The sea ice cover has decreased to a minimal extent in the summers of 2002–2005 as observed with satellite microwave data [*Sturm et al.*, 2003; *Francis et al.*, 2005; *Nghiem*, 2005; *Stroeve et al.*, 2005]. Since the 1970s, summer ice extent has reduced at a long-term rate of 6.4–7.8% per decade [*Comiso*, 2002; *Francis et al.*, 2005]. A diminished sea ice cover may profoundly impact the Arctic environment and ecosystem, transportation and commerce, resource development, marine operations, and national security [*Office of Naval Research et al.*, 2001; *Nghiem*, 2004; *Wilson et al.*, 2004; *Grebmeier*, 2005].

[3] To monitor sea ice over the Arctic Ocean, two types of satellite microwave data have been used on a daily basis: passive microwave radiometer and active microwave scatterometer. While both sensors can measure the extent of the total sea ice cover, passive microwave data have been used to estimate ice concentration [*Cavalieri et al.*, 1984; *Comiso*, 1995; *Markus and Cavalieri*, 2000; *Partington*, 2000] and active microwave data are appropriate to delineate and map sea ice classes. Early research was carried out to investigate the use of passive microwave data for sea ice classification [*Eppler et al.*, 1986]; however, there are significant uncertainties in passive microwave results [*Maslanik*, 1992; *Thomas*, 1993]. The capability of Ku-band scatterometer to map sea ice, including the multi-year ice class, was demonstrated and results for Arctic sea ice were published [*Kwok et al.*, 1999; *Nghiem and Neumann*, 2002; *Nghiem*, 2004; *Nghiem et al.*, 2005].

[4] Arctic sea ice consists of two major classes: perennial or multi-year sea ice defined as sea ice that survives at least one summer and can be as thick as 3 m or more [*Armstrong et al.*, 1973], and seasonal or first-year sea ice that grows in the current freezing season and is significantly thinner (0.3–2 m) [*Armstrong et al.*, 1973] than perennial ice. In this paper, we present new observations of recent anomalous change in: (1) the distribution of these sea ice classes, and (2) the significant reduction of perennial ice over the Arctic Ocean in the fall of 2005 to the spring of 2006, compared to sea ice conditions in November–December 2004, rather than just minimal sea ice extent in summertime as previously reported [*Sturm et al.*, 2003; *Nghiem*, 2004, 2005; *Stroeve et al.*, 2005]. The capability to monitor change in both extent and distribution of different ice classes especially perennial ice in fall, winter, and spring provides crucial information to address change in Arctic ice mass balance.

2. Approach

[5] We use scatterometer data acquired by the U.S. National Aeronautics and Space Administration (NASA) SeaWinds scatterometer on board the QuikSCAT satellite (QSCAT). This satellite was launched in June 1999 and has been continuously collecting data over the world. The QSCAT sensor measures backscatter at horizontal (*HH*) and vertical (*VV*) polarizations with the respective swaths of 1400 and 1800 km [*Tsai et al.*, 2000] allowing a coverage of the Arctic region twice per day. We developed a robust algorithm to detect and map Arctic sea ice from QSCAT data [*Nghiem and Neumann*, 2002; *Nghiem*, 2004, 2005; *Nghiem et al.*, 2005]. The QSCAT algorithm utilizes both *HH* and *VV* polarizations and multi-azimuth looks in the data set. This algorithm employs a data-pairing method to achieve a strict collocation of data in time and space. It identifies sea ice from open water based on polarization signatures, azimuth asymmetry, and differences in backscatter stability and consistency over sea ice versus open water. The robustness of this algorithm for ice detection over a wide range of wind speed has been published [*Nghiem et al.*, 2005].

[6] Within the ice cover, seasonal and perennial ice classes have distinctive backscatter signatures. The fundamental electromagnetic scattering physics was studied from the first principles and published by *Nghiem et al.* [1995a, 1995b] based on different physical characteristics in salinity,

[1]Jet Propulsion Laboratory, California Institute of Technology, Pasadena, California, USA.
[2]U.S. Army Cold Region Research and Engineering Laboratory, Hanover, New Hampshire, USA.
[3]National Ice Center, Washington, DC, USA.

Copyright 2006 by the American Geophysical Union.
0094-8276/06/2006GL027198$05.00

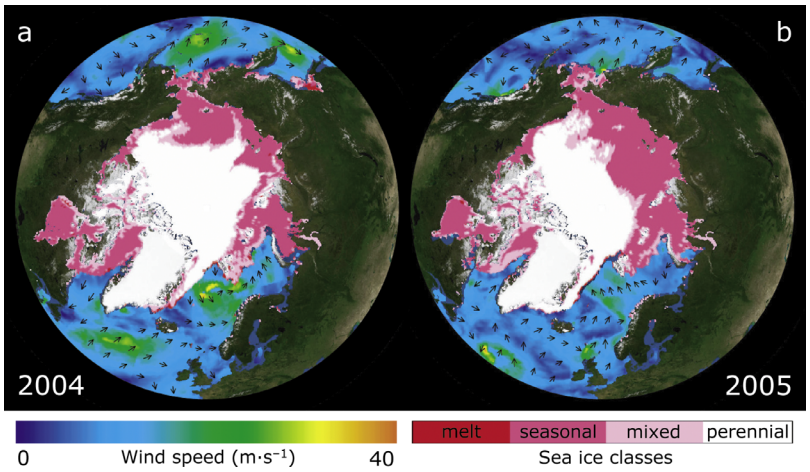

Figure 1. Arctic sea ice and wind vectors measured by QSCAT on (a) 21 December 2004 and (b) 21 December 2005. The sea ice classes include perennial or multi-year ice (white), mixed ice (pink), and seasonal or first-year ice (magenta). Over ice-free oceans, wind speed is plotted from 0 $m \cdot s^{-1}$ (blue) to 40 $m \cdot s^{-1}$ (orange) and wind direction is represented by arrows. Land is denoted with the NASA 1-km land data set.

porosity, layering, and surface properties of different ice types [*Weeks and Ackley*, 1982; *Wen et al.*, 1989]. In fact, analyses of satellite scatterometer data showed a large dynamic range of Ku-band backscatter and thus a strong sensitivity to the different classes from seasonal (first-year) to perennial (multi-year) ice [*Ezraty and Cavanié*, 1999]. We have developed a sea ice classification algorithm based on statistical analysis showing two separate distinctive peaks in backscatter data for seasonal and perennial sea ice in freezing seasons [*Nghiem and Neumann*, 2002; *Nghiem*, 2004, 2005]. There is an overlap between seasonal and perennial ice backscatter, which is used to identify the mixed sea ice class consisting of a mixture of different forms of first-year and multi-year ice. When first-year ice is compressed, the ice can be significantly thickened and roughened by rafting and ridging, and also desalinated by brine drainage. This kind of first-year ice is similar to multi-year ice in physical properties and backscatter signature, and we include this ice type in the class of mixed ice. We verify QSCAT results with observations from a field validation campaign using the U.S. Coast Guard icebreaker, the USCGC Healy, over the Barents Sea in October–November 2001 [*Nghiem*, 2003; *Nghiem et al.*, 2005].

[7] QSCAT was originally designed to measure wind speed and wind direction over ice-free ocean surfaces. The QSCAT wind retrieval algorithm uses QSCAT data at multiple azimuth angles based on a geophysical model function relating backscatter to wind speed and direction as a function of azimuth angle, incidence angle, and polarization [*Tsai et al.*, 2000]. The nominal accuracy of QSCAT wind results is the larger of 2 $m \cdot s^{-1}$ or 10% for wind speed from 3 to 30 $m \cdot s^{-1}$, and 20° for wind direction [*Lungu*, 2001]. Thus, QSCAT can monitor both the wind field and sea ice, which are crucial for ice forecasting especially in anomalous conditions.

3. Results

[8] The maps in Figure 1 present sea ice extent, ice classes, and ocean wind vectors over the Arctic Ocean on the winter solstice days of 21 December 2004 (Figure 1a) and 21 December 2005 (Figure 1b). We use NASA's 1-km global imagery (NASA Goddard Space Flight Center, The Blue Marble: True-color global imagery at 1 km resolution, Earth Observatory News, available at http://earthobservatory.nasa.gov/Newsroom/BlueMarble/BlueMarble_2002.html) to represent the land cover in Figure 1. The sea ice cover consists of three classes: perennial, mixed, and seasonal sea ice. Over an ice-free ocean, a color scale from blue to orange denotes wind speed. The arrows delineate wind direction plotted at every 6° in longitude and latitude to avoid overcrowding the images with wind vectors. We project the Earth image into a spherical coordinate with a composite image of ice and wind overlaid on the map.

[9] In this paper, we define the East Arctic Ocean as the Arctic Ocean occupying 0° to 180°E longitudes, and the West Arctic Ocean as 0° to 180°W longitudes. Figure 1a (2004 winter solstice) shows that perennial sea ice cover dominated Arctic sea ice spanning the West Arctic Ocean and protruding well into the Laptev Sea and the northwest region of the East Siberian Sea (east of the New Siberian Islands) in the East Arctic Ocean. Seasonal sea ice occupied the Hudson Bay, the Baffin Bay, the Canadian Arctic archipelago, the Beaufort and Chukchi Seas in the West Arctic Ocean, and parts of the Barents, Kara, Laptev, and East Siberian Seas in the East Arctic Ocean. The mixed ice class is typically observed at the boundary between seasonal and perennial ice as expected. However, the perennial ice extent in 2004 compared to QSCAT results in the winters of 2000–2003 had further decreased in the Beaufort, Chukchi, and East Siberian Seas, suggesting a decreasing trend in Arctic perennial sea ice extent over these recent years [*Nghiem et al.*, 2006]. In earlier years, the largest change occurred also in the Beaufort and Chukchi Seas [*Comiso*, 2002].

[10] Figure 1b presents the distribution of sea ice classes over the Arctic Ocean on the winter solstice in 2005. There are two striking observations: (1) a large decrease in the total extent of perennial sea ice, and (2) a confinement of perennial ice largely to the West Arctic Ocean leaving the East Arctic Ocean occupied mostly by seasonal sea ice. The perennial sea ice that had extended into the Laptev Sea and

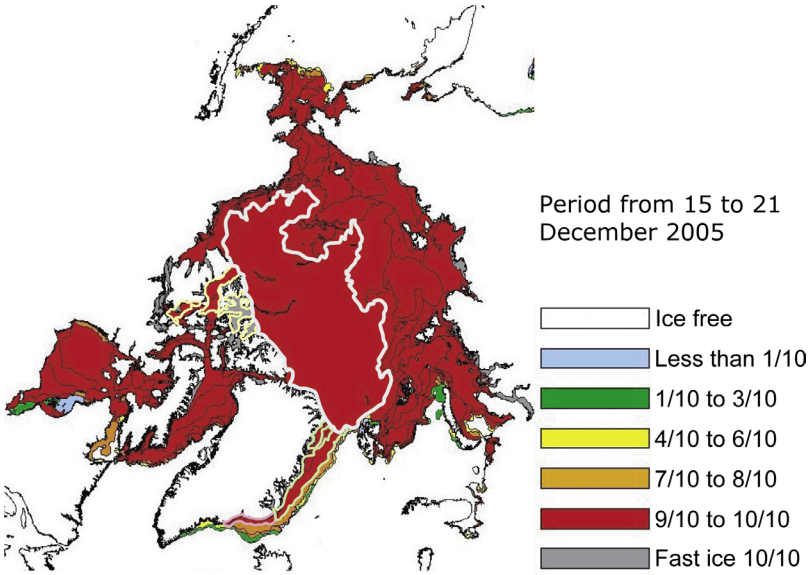

Figure 2. Arctic sea ice chart prepared by the U.S. National Ice Center with various satellite data sets collected in the period 15–21 December 2005. Ice concentration from ice free to full pack ice (10/10) is denoted with different colors. Black contours represent ice areas with different characteristics according to the World Meteorological Organization system. Light-grey contour marks the dominant multi-year ice pack in the West Arctic Ocean. Light-green contour is for the east Greenland area dominated by multi-year ice, and pink contour contains 40% multi-year ice. Light-yellow contour indicates multi-year ice areas in the Canadian Arctic Archipelago.

part of the East Siberian Sea in 2004 (Figure 1a) totally disappeared in 2005 (Figure 1b). In the Baffin Bay, a large area is identified as mixed ice (Figure 1b) containing rafted and ridged ice due to ice compression as discussed in section 2. In both images in Figure 1, QSCAT identifies the ice along the east coast of Greenland as multi-year (perennial) ice. The area between Greenland and Spitsbergen is well known as the Fram Strait region, where sea ice is dominated by multi-year ice and some multi-year ice can be as old as 5 years [*Gow et al.*, 1987; *Gow and Tucker*, 1987; *Tucker et al.*, 1987]. Thus, the perennial ice result from QSCAT data is consistent with multi-year ice observed in this region east of Greenland.

[11] To compare the drastic change observed by QSCAT in 2005, we present in Figure 2 an Arctic sea ice chart for the period 15–21 December 2005. Analysts at the U.S. National Ice Center (NIC) manually prepare an Arctic ice chart once every two weeks based on various satellite data sources. The NIC ice chart depicts sea ice concentration, defined as the fraction of the sea surface covered by ice, ranging from ice-free conditions to mostly ice covered. Moreover, black contour lines on the NIC ice chart mark local areas that are characterized by stages of ice development and predominant form of ice (floe size) according to the World Meteorology Organization system for sea ice symbology [*World Meteorological Organization*, 2004]. Data used to obtain the ice chart in Figure 2 consist of 43% from the Defence Meteorological Satellite Program Operational Linecan System, 31% from RADARSAT Synthetic Aperture Radar (SAR), 11% from Envisat SAR, 6% from Moderate Resolution Imaging Spectroradiometer and from Advanced Very High Resolution Radiometer, and only 7% from QuikSCAT; therefore, the NIC ice chart is primarily an independent result derived from different data sets with a different approach. Despite these differences and the data dates, the NIC ice chart reveals the similarity of the West Arctic dominant ice pack (light-grey contour in Figure 2) both in size and in shape compared to the 2005 QSCAT perennial ice pack (white area in Figure 1b), and thus independently cross-verifies the results. In further details (Figure 2), the light-green contour in the Greenland Sea contains multi-year ice and the light-yellow contour in the Canadian Arctic Archipelago represents fast ice surviving the 2005 summer. Except for the small pink-contour area stretched along the southeast coast of Greenland where NIC shows only 40% multi-year ice concentration, NIC and QSCAT results are in a good agreement.

[12] To carry out a quantitative analysis, we obtained daily sea ice cover maps over periods of 2 months from 1 November to 31 December in 2004 and in 2005. In each time period, the general sea ice distribution is similar to that on the winter solstice day in Figure 1 for each year. In November and December, the sea ice pack was stable and the ice cover was under freezing conditions. We note that QSCAT backscatter is sensitive to surface melt and we use QSCAT data to detect and map sea-ice melt zones based on a diurnal change approach [*Nghiem et al.*, 2001; *Nghiem and Neumann*, 2002]. We actually identify melt as another ice class (red pixels in Figure 1; e.g., at the ice edge east of Greenland) in addition to the perennial, seasonal, and mixed ice classes. For each day, we calculate the surface area of each ice class. In 2004 and 2005, daily results indicate that the total area of perennial ice was stable with little change during November–December of each year. In contrast, the change of perennial sea ice extent between the two years is large: a decrease of 0.72×10^6 km^2 in surface area of the perennial ice extent averaged over November–December in 2005 compared to that in 2004. This reduced area is about the size of the State of Texas, the largest state in the conterminous United States. This change is about 14%

Table 1. Sea Ice Extent in 2004 and 2005 (Start Value on 1 November, Mean Value, and End Value on 31 December) and the Difference (Mean and Standard Deviation) Between Two Years Over the Months of November and December[a]

Ice Class	Year	East Arctic	West Arctic	All Arctic
Perennial sea ice	2004	2.20, 2.00, 1.67	3.00, 3.10, 3.16	5.19, 5.09, 4.83
	2005	1.34, 1.05, 0.89	3.15, 3.32, 3.47	4.49, 4.37, 4.36
	Difference	−0.95 ± 0.08	0.23 ± 0.06	−0.72 ± 0.10
Seasonal sea ice	2004	1.67, 2.14, 2.67	0.81, 1.86, 2.87	2.48, 4.01, 5.54
	2005	2.33, 3.03, 3.41	0.66, 1.59, 2.59	2.99, 4.62, 6.01
	Difference	0.88 ± 0.13	−0.27 ± 0.13	0.61 ± 0.17
All ice classes	2004	4.56, 5.03, 5.26	4.79, 6.30, 7.50	9.35, 11.3, 12.8
	2005	4.52, 4.80, 5.17	4.78, 6.32, 7.63	9.30, 11.1, 12.8
	Difference	−0.23 ± 0.18	0.02 ± 0.15	−0.21 ± 0.19

[a]A negative (positive) mean value of the difference indicates a decrease (increase) of ice extent in 2005. The unit is 10^6 km^2.

decrease within one year, which is 18 times larger that the long-term rate of 7.8% per decade [*Francis et al.*, 2005]. Data from the National Centers for Environmental Prediction/National Center for Atmospheric Research (NCEP/NCAR) reanalysis reveal a strong northerly wind anomaly over the Greenland Sea during summer 2005 (July–September) responsible for anomalous ice export through the Fram Strait. Daily QSCAT results also show a consistent increase in the total ice extent due to sea ice growth during November–December in 2004 and in 2005. Averaged over these two months, the total area of all Arctic sea ice in 2005 was nearly unchanged with a modest decrease of about 0.21×10^6 km^2 (only 1.9% change) compared to that in 2004 (Table 1), indicating that most of the areal reduction in perennial ice was replaced by seasonal ice.

[13] We partition QSCAT data into west and east longitudes to investigate the change in sea ice distribution between the East and the West Arctic Oceans during November–December in 2004 and in 2005. Table 1 summarizes the results for these two regions and also for the entire Arctic Ocean. In the East Arctic Ocean, nearly half (48%) of perennial sea ice extent disappeared with an anomalous reduction of 0.95×10^6 km^2 in 2005 from a perennial ice extent of 2.00×10^6 km^2 in 2004. The change of 48% within one year is abrupt compared to the long-term rate of 7.8% per decade for total summer ice reduction [*Francis et al.*, 2005]. In the West, the perennial ice extent had a gain of 0.23×10^6 km^2, four times smaller compared to the loss in the East Arctic perennial ice extent. This differential change resulted in the large decrease in the net perennial ice extent over the entire Arctic Ocean in 2005 (Table 1). Most of the reduction of perennial ice extent in the East Arctic Ocean was reoccupied by seasonal ice grown in the 2005 freezing season. Thus, while the total sea ice extent had little change between 2004 and 2005 (November–December), there was a very large imbalance in perennial and seasonal ice distribution between the East and the West Arctic Oceans.

[14] The perennial ice continued to be depleted from the East Arctic Ocean. Figure 3 presents the drastic reduction of perennial ice extent between October 2005 and the recent condition in April 2006. The plot of daily perennial ice extent reveals a steep decrease in the East Arctic. Short-term changes or fluctuations in ice areas were caused by ice divergence and convergence, and by wind-driven shifts in the distribution of seasonal and perennial ice between the East and the West Arctic Oceans. On 1 October 2005, perennial ice occupied 1.49×10^6 km^2 in the East and 3.15×10^6 km^2 in the West. By 15 April 2006, perennial ice in the East Arctic Ocean was mostly depleted with a remaining area of only 0.45×10^6 km^2 (70% reduction), while perennial ice in the West slightly increased to 3.45×10^6 km^2 (9.5% gain). This result suggests an excessive migration of perennial ice from the East to the West Arctic compared to the perennial ice export out of the West Arctic. NCEP/NCAR reanalysis data show: (1) zonal winds blowing from east to west over the Beaufort Sea pulling perennial ice into this sea, (2) meridional winds blowing from north to south over the Greenland Sea exporting ice through the Fram Strait, and (3) wind forcing from the East to the West Arctic Ocean pushing the perennial ice pack toward the West Arctic. Wind effects (1) and (2) made space for (3) to move perennial ice into the West and thus depleting it from the East Arctic Ocean.

4. Discussion

[15] Since 2002, the total sea ice extent in summer months remained at or near record minimum [*Sturm et al.*, 2003;

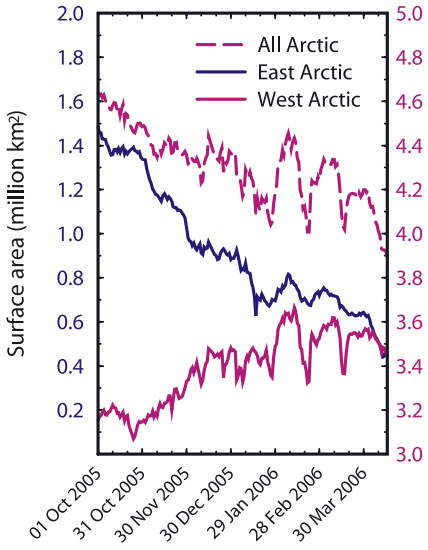

Figure 3. Areas of perennial sea ice extent in all Arctic, East Arctic (0–180°E) and West Arctic (0–180°W) Ocean from 1 October 2005 to 15 April 2006 as observed by QSCAT. Each color scale on the vertical axis applies to the plot with the same color.

Nghiem, 2004, 2005; *Stroeve et al.*, 2005; *Nghiem et al.*, 2006] indicating that most of the seasonal ice could not sufficiently survive summer conditions to regain the coverage before 2002. If this trend continues, most of the seasonal ice (magenta areas in Figure 1b) may be removed by summer melt, enhanced solar energy input, ice export, and wind-ocean-ice interactions. These effects potentially open a vast region of ice-free ocean in the East Arctic Ocean leading to another record minimum of summer sea ice extent.

[16] On the 2006 spring equinox (21 March 2006), the boundary of perennial ice extent (image not shown here) moved further toward the West Arctic Ocean compared to that on the last winter solstice (21 December 2005, Figure 1b). If the sea ice edge would form near this boundary in the coming summer, the ice extent would have retreated away from the East Arctic continental shelf resulting in more effective ocean mixing and ice interactions [*Carmack and Chapman*, 2003; *Nghiem et al.*, 2005]. Moreover, the ice-free ocean reflects less than 10% of the incident solar radiation compared to approximately 40 to 50% reflected by melting perennial ice (D. K. Perovich et al., Seasonal evolution and interannual variability of the solar energy absorbed by the Arctic sea ice-ocean system, submitted to *Journal of Geophysical Research*, 2005). In addition, the albedo of melting seasonal ice is less than that of melting perennial ice. As a result, substantially more solar radiation would be absorbed into the ice-ocean system, both accelerating summer melt and impeding fall freeze-up. Consequently, the lengthened melt season would further diminish the Arctic ice cover. For ice modelling, new results from scatterometer data are important to be assimilated into model such as the Community Climate System Model [*Weatherly et al.*, 2005] to study Arctic environmental change.

[17] Unlike the emphasis in past results on just the decrease of perennial ice extent, it should be noted that not only the large reduction in the extent of total Arctic perennial ice but also the depletion of this ice class from the East Arctic Ocean could have a significant impact on Arctic environment and maritime operations. Nevertheless, the recent anomalous change in the Arctic Ocean is not well understood and thus any long-range forecast of Arctic environmental change may have a large uncertainty. This fact emphasizes the need for an Arctic integrated information system that combines satellite monitoring of ice and ocean together with environmental data from surface measurement networks. The timely dissemination of Arctic information through the Internet to researchers, mariners, local residents and policy planners is important to both scientific studies and operational applications. As a demonstration, we have developed an initial system using QSCAT data to simultaneously monitor ice conditions (over sea ice) and ocean wind vectors (over ice-free water 25 km away from the ice edge) in the Bering, Chukchi, Beaufort, and East Siberian Seas [*Nghiem et al.*, 2006] (see Animation S1 in the auxiliary material[1] and also results available at http://ourocean.jpl.nasa.gov/beringsea.html). This demonstration can be transitioned to routine operations providing near-real-time ice-ocean monitoring and forecast capabilities to meet growing research needs and application interests.

[1]Auxiliary materials are available in the HTML. doi:10.1029/2006GL027198.

[18] **Acknowledgments.** The research carried out by the Jet Propulsion Laboratory, California Institute of Technology, and by the Engineer Research and Development Center, Cold Region Research and Engineering Laboratory, was supported under a contract with NASA. The views, opinions, and findings contained in this report are those of the authors and should not be construed as an official National Oceanic and Atmospheric Administration, or any other U.S. government position, policy, or decision.

References

Armstrong, T., B. Roberts, and C. Swithinbank (1973), *Illustrated Glossary of Snow and Ice*, 2nd ed., Scott Polar Res. Inst., Cambridge, U. K.

Carmack, E., and D. C. Chapman (2003), Wind-driven shelf/basin exchange on an Arctic shelf: The joint roles of ice cover extent and shelf-break bathymetry, *Geophys. Res. Lett.*, *30*(14), 1778, doi:10.1029/2003GL017526.

Cavalieri, D. J., P. Gloersen, and W. J. Campbell (1984), Determination of sea ice parameters with the Nimbus 7 scanning multichannel microwave radiometer, *J. Geophys. Res.*, *89*, 5355–5369.

Comiso, J. C. (1995), SSM/I concentrations using the bootstrap algorithm, *NASA Rep.*, *1380*, 40 pp.

Comiso, J. (2002), A rapidly declining perennial sea ice cover in the Arctic, *Geophys. Res. Lett.*, *29*(20), 1956, doi:10.1029/2002GL015650.

Eppler, D. T., L. D. Farmer, A. W. Lohanick, and M. Hoover (1986), Classification of sea ice types with single-band (33.6 GHz) airborne passive microwave imagery, *J. Geophys. Res.*, *91*, 661–695.

Ezraty, R., and A. Cavanié (1999), Intercomparison of backscatter maps over Arctic sea ice from NSCAT and the ERS scatterometer, *J. Geophys. Res.*, *104*, 11,471–11,483.

Francis, J. A., E. Hunter, J. R. Key, and X. Wang (2005), Clues to variability in Arctic minimum sea ice extent, *Geophys. Res. Lett.*, *32*, L21501, doi:10.1029/2005GL024376.

Gow, A. J., and W. B. Tucker (1987), Physical properties of sea ice discharged from Fram Strait, *Science*, *236*(4800), 436–439.

Gow, A. J., W. B. Tucker, and W. F. Weeks (1987), Physical properties of summer sea ice in the Fram Strait, June–July 1984, *Rep. 87-16*, 81 pp., Cold Reg. Res. Eng. Lab., Hanover, N. H.

Grebmeier, J. A. (2005), The Western Arctic Shelf-Bain Interactions (SBI) project: An overview, *Deep Sea Res., Part II*, *52*, 3109–3115.

Kwok, R., G. F. Cunningham, and S. Yueh (1999), Area balance of the Arctic Ocean perennial ice zone: October 1996 to April 1997, *J. Geophys. Res.*, *104*, 25,747–25,759.

Lungu, T., (Ed.) (2001), QuikSCAT science data product user's manual, *Doc. D-18053*, 95 pp., Jet Propul. Lab., Pasadena, Calif.

Markus, T., and D. J. Cavalieri (2000), An enhancement of the NASA Team sea ice algorithm, *IEEE Trans. Geosci. Remote Sens.*, *38*, 1387–1398.

Maslanik, J. A. (1992), Effects of weather on the retrieval of sea ice concentration and ice type from passive microwave data, *Int. J. Remote Sens.*, *13*(1), 37–54.

Nghiem, S. V. (2003), Arctic field validation campaign for satellite remote sensing of sea ice, *Doc. D-26211*, 44 pp., Jet Propul. Lab., Pasadena, Calif.

Nghiem, S. V. (2004), Observations of Arctic environmental change, in *Proceedings 2004 IEEE International Geoscience and Remote Sensing Symposium, 2004: IGARSS '04*, volume II, page 1322, IEEE Press, Piscataway, N. J.

Nghiem, S. V. (2005), Space-borne Ku-band radar observations of extreme surface water conditions, *Eos Trans. AGU*, *86*(52), Fall Meet. Suppl., Abstract H21D-1381.

Nghiem, S. V., and G. Neumann (2002), Snow and ice in the Earth system viewed by space scatterometer observatory, *Eos Trans. AGU*, *83*(47), Fall Meet. Suppl., Abstract C72B-02.

Nghiem, S. V., R. Kwok, S. H. Yueh, and M. R. Drinkwater (1995a), Polarimetric signature of sea ice: 1. Theoretical model, *J. Geophys. Res.*, *100*, 13,665–13,679.

Nghiem, S. V., R. Kwok, S. H. Yueh, and M. R. Drinkwater (1995b), Polarimetric signature of sea ice: 2. Experimental observations, *J. Geophys. Res.*, *100*, 13,681–13,698.

Nghiem, S. V., K. Steffen, R. Kwok, and W.-Y. Tsai (2001), Detection of snowmelt regions on the Greenland ice sheet using diurnal backscatter change, *J. Glaciol.*, *47*, 539–547.

Nghiem, S. V., M. L. Van Woert, and G. Neumann (2005), Rapid formation of a sea ice barrier east of Svalbard, *J. Geophys. Res.*, *110*, C11013, doi:10.1029/2004JC002654.

Nghiem, S. V., Y. Chao, E. Rodriguez, P. Li, G. Neumann, D. K. Perovich, J. W. Weatherly, P. Clemente-Colón, H. Eicken, and A. Mahoney (2006), Arctic sea ice and ocean monitoring with satellite scatterometer, *Eos Trans. AGU*, *87*(36), Ocean Sci. Meet. Suppl., Abstract OS11A-05.

Office of Naval Research, Naval Ice Center, Oceanographer of the Navy, and the Arctic Research Commission (2001), Naval operations in an ice

free arctic, final report of the Naval Operations in and Ice-free Arctic Symposium, Off. of Nav. Res., Washington, D. C.

Partington, K. C. (2000), A data fusion algorithm for mapping sea-ice concentrations from Special Sensor Microwave/Imager data, *IEEE Trans. Geosci. Remote Sens.*, *38*, 1947–1958.

Stroeve, J. C., M. C. Serreze, F. Fetterer, T. Arbetter, W. Meier, J. Maslanik, and K. Knowles (2005), Tracking the Arctic's shrinking ice cover: Another extreme September minimum in 2004, *Geophys. Res. Lett.*, *32*, L04501, doi:10.1029/2004GL021810.

Sturm, M., D. K. Perovich, and M. C. Serreze (2003), Meltdown in the north, *Sci. Am.*, *288*, 60–67.

Thomas, D. R. (1993), Arctic sea-ice signatures for passive microwave algorithms, *J. Geophys. Res.*, *98*, 10,037–10,052.

Tsai, W.-Y., S. V. Nghiem, J. N. Huddleston, M. W. Spencer, B. W. Stiles, and R. D. West (2000), Polarimetric scatterometry: A promising technique for improving ocean surface wind measurements, *IEEE Trans. Geosci. Remote Sens.*, *38*, 1903–1921.

Tucker, W. B., A. J. Gow, and W. F. Weeks (1987), Physical properties of summer sea ice in the Fram Strait, *J. Geophys. Res.*, *92*, 6787–6804.

Weatherly, J. W., D. K. Perovich, and S. V. Nghiem (2005), Variability in the Arctic sea ice melt season, J6.7, paper presented at 85th American Meteorological Society Meeting, San Diego, Calif.

Weeks, W. F., and S. F. Ackley (1982), The growth, structure, and properties of sea ice, *CRREL Monogr. 82-1*, Cold Regions Res. Eng. Lab., Hanover, N. H.

Wen, T., W. J. Felton, J. C. Luby, W. L. J. Fox, and K. L. Kientz (1989), Environmental measurements in the Beaufort Sea, *Tech. Rep. APL-UW TR 8822*, Appl. Phys. Lab., Univ. of Wash., Seattle.

Wilson, K. J., J. Falkingham, H. Melling, and R. De Abreu (2004), Shipping in the Canadian Arctic—Other possible climate change scenarios, in *Proceedings 2004 IEEE International Geoscience and Remote Sensing Symposium, 2004: IGARSS '04*, volume III, pages 1853–1856, IEEE Press, Piscataway, N. J.

World Meteorological Organization (2004), Ice chart colour code standard, *Rep. WMO/TD-1215*, Geneva, Switzerland.

Y. Chao, P. Li, G. Neumann, and S. V. Nghiem, Jet Propulsion Laboratory, California Institute of Technology, MS 300-325, 4800 Oak Grove Drive, Pasadena, CA 91109, USA. (son.v.nghiem@jpl.nasa.gov)

P. Clemente-Colón and T. Street, National Ice Center, Federal Building 4, 4251 Suitland Road, Washington, DC 20395, USA.

D. K. Perovich, U.S. Army Cold Regions Research and Engineering Laboratory, 72 Lyme Road, Hanover, NH 03755-1290, USA.